Journal of Photonics for Energy

PhotonicsforEnergy.SPIEDigitalLibrary.org

Fabrication of highly reproducible polymer solar cells using ultrasonic substrate vibration posttreatment

Yu Xie
Fatemeh Zabihi
Morteza Eslamian

SPIE.

Yu Xie, Fatemeh Zabihi, Morteza Eslamian, "Fabrication of highly reproducible polymer solar cells using ultrasonic substrate vibration posttreatment," *J. Photon. Energy* **6**(4), 045502 (2016), doi: 10.1117/1.JPE.6.045502.

Fabrication of highly reproducible polymer solar cells using ultrasonic substrate vibration posttreatment

Yu Xie, Fatemeh Zabihi, and Morteza Eslamian*
University of Michigan-Shanghai Jiao Tong University Joint Institute, UM-SJTU Joint Institute Building, 800 Dongchuan Road, Minhang District, Shanghai 200240, China

Abstract. Organic solar cells are usually nonreproducible due to the presence of defects in the structure of their constituting thin films. To minimize the density of pinholes and defects in PEDOT:PSS, which is the hole transporting layer of a standard polymer solar cell, i.e., glass/ITO/PEDOT:PSS/P3HT:PCBM/Al, and to reduce scattering in device performance, wet spun-on PEDOT:PSS films are subjected to imposed ultrasonic substrate vibration posttreatment (SVPT). The imposed vibration improves the mixing and homogeneity of the wet spun-on films, and consequently the nanostructure of the ensuing thin solid films. For instance, our results show that by using the SVPT, which is a mechanical, single-step and low-cost process, the average power conversion efficiency of 14 identical cells increases by 25% and the standard deviation decreases by 22% indicating that the device photovoltaic performance becomes more consistent and significantly improved. This eliminates several tedious and expensive chemical and thermal treatments currently performed to improve the cell reproducibility. [DOI: 10.1117/1.JPE.6.045502]

Keywords: organic solar cells; polymer solar cells; poly(3,4-ethylenedioxythiophene) polystyrene sulfonate; imposed ultrasonic substrate vibration; reproducible solar cells.

Paper 16067 received Jun. 1, 2016; accepted for publication Oct. 11, 2016; published online Nov. 3, 2016.

1 Introduction

Owing to their potential in low-cost fabrication, solution-processed solar cells, represented by polymer solar cells, are promising alternatives to the widely commercially used crystalline silicon-based and inorganic thin film solar cells.[1,2] Polymer solar cells conceptually work based on electron/hole generation in a donor/acceptor (D/A) system when exposed to sunlight (the photovoltaic effect),[3] in which excitons generated in donor by absorbing photons diffuse to the D/A interface and therein dissociate into electrons and holes. Electrons and holes are then guided toward the opposite electrodes using buffer layers. Because of the short diffusion length of excitons, which is on the order of 10 nm,[4,5] modern polymer solar cells use the concept of bulk heterojunction,[6,7] in which donor and acceptor materials are mixed together, interpenetrating at the nanometer scale, and forming a thin film active layer. Blend of poly(3-hexylthiophene) (P3HT) and phenyl-C61-butyric acid methyl ester (PCBM) as a standard heterojunction D/A system has attracted intense attention, mainly in the conventional cell architecture, i.e., glass/ITO/PEDOT:PSS/P3HT:PCBM/Al, where indium-doped thin oxide (ITO) and Al serve as the anode and cathode, respectively. Poly(3,4-ethylenedioxythiophene) polystyrene sulfonate (PEDOT:PSS) is a conducting polymer mixture of two ionomers, which has the role of hole extraction from the active layer and blocks electron transfer.

Achieving proper nanostructure for the mixture of P3HT:PCBM and similar polymer systems is essential for effective charge generation, dissociation, and transfer. Thermal annealing has been widely applied to solar cells with a D/A system of P3HT:PCBM to arrange the nanostructure properly and to improve the photovoltaic performance.[3,8–10] The enhancement in

*Address all correspondence to: Morteza Eslamian, E-mail: Morteza.Eslamian@sjtu.edu.cn

Table 1 Typical reported PCE of P3HT:PCBM polymer solar cells.

Cell architecture	Fabrication method	Effective area (cm^2)	Best PCE (%)	Lowest PCE (%)	Reference
ITO/PEDOT:PSS/ P3HT:PCBM/Ca/Al	Spin coating	0.11	4	—	3
ITO/PEDOT:PSS/ P3HT:PSS/ZnO/Al	Inkjet printing	1	2.7	—	18
ITO/PEDOT:PSS/ P3HT:PCBM/Al	Slot-die	1	2.72	2.0	19
ITO/PEDOT:PSS/ P3HT:PCBM/Ca/Al	Spraying	0.164	2.83	—	20

photovoltaic performance has been attributed to the improvement made in the crystalline structure of P3HT, leading to higher hole mobility[11,12] and phase separation between P3HT and PCBM domains during thermal annealing. The optimal thermal annealing conditions vary with the film thickness and the ratio of P3HT to PCBM. Nevertheless, the annealing temperature is usually in the range of 110 to 150°C and the annealing time is less than 45 min.[3,10–12] It is noted that although P3HT:PCBM is the standard and most studied D/A system, other polymer blends with lower bandgaps have also been used to obtain compelling photovoltaic performance.[13–17] In this fundamental study, however, the P3HT:PCBM system is used, while the findings may be extended to solar cells with similar architecture.

Table 1 lists the power conversion efficiency (PCE) of several solar cells based on P3HT:PCBM system, reported in the literature. As listed in Table 1, for the spun-on cells with the architecture ITO/PEDOT:PSS/P3HT:PCBM/Ca/Al, after optimization of the active layer thickness, and thermal annealing, the best PCE of 4% has been achieved.[3] However, the performance of other cells fabricated under the same conditions was not reported, thus the reproducibility of the process cannot be evaluated. Furthermore, for the best PCE reported in Table 1, the performance data were extracted from a cell with an effective area of 0.1 cm^2. While obtaining a highly uniform spun-on film with a small area is less challenging, scaling up of the technology entails the fabrication of cells with larger areas or the fabrication of multiple cells on a large-area substrate to connect the cells for higher voltage and current. Table 1 also shows the PCE of solar cells fabricated using scalable methods, such as inkjet printing,[18] slot-die,[19] and spray coating,[20] with various active layer areas. Only in the case of the cell fabricated by slot-die printing, the lowest efficiency as well as the highest efficiency are reported. Table 1 shows that the PCE of the cells made by scalable methods is generally lower than those of the cells made by spin coating, given that the films with larger area and made by scalable methods are less uniform and have a higher density of pinholes.

As far as the scaling up of the technology is concerned, several strategies may be followed: development of scalable coating and printing methods, such as screen printing,[21] inkjet printing,[18,22] slot-die coating,[19] and spray coating,[23,24] customized and optimized for solar cell technology is an important step to achieve uniform and defect-free large-area thin films and devices with compelling performance. Also, when several cells are made on a substrate, usually a few cells which have a uniform and defect-free structure, show an acceptable performance, and the rest of the cells actually do not show any power output or show low performance. Therefore, to pave the way for commercialization of polymer and other solution-processed solar cells, the development of scalable coating techniques, as well as the development of treatments and strategies for the fabrication of multiple defect-free and reproducible cells on a larger substrate is essential. By reproducible or repeatable cells, it is meant that devices which are made under the same fabrication route shall show very similar performances. Here, to better tackle the problem and address one issue at a time, the lab-scale spin coating method is employed and an attempt is made to fabricate multiple reproducible devices on a substrate. To this end, wet spun-on films (in this work, PEDOT:PSS films) are placed on a substrate that is ultrasonically vibrated in the vertical direction,[25–29] a method we have recently developed. The imposed substrate vibration

technique was tested on drop-cast perovskite solar cells,[25] spray-on polymer thin films,[26,27] spun-on polymer films,[28] and spray-on perovskite solar cells,[29] where the remarkable positive impact on the nanostructure and functionality of the thin films and the device performance were achieved. In this work, the glass/ITO/PEDOT:PSS/P3HT:PCBM/Al structure is used as the model polymer solar cell. In most of literature works, a thin layer of Ca is deposited below the Al layer to tune the work function and improve the device performance. However, in this work, Ca layer is eliminated due to technical difficulties associated with the deposition of Ca, which is a highly reactive metal and is not in line with large-scale and low-cost fabrication of the organic solar cells. The P3HT:PCBM and PEDOT:PSS layers are deposited by spin coating; however, the as-spun wet PEDOT:PSS layer is subjected to ultrasonic substrate vibration posttreatment (SVPT).[28] The results show that this simple treatment makes the fabrication process highly reproducible.

2 Materials and Methods

Figure 1 shows the schematic of the spin coating process, followed by the SVPT, which is used to fabricate PEDOT:PSS thin films atop ITO-coated glass substrates (24 mm × 24 mm, sheet resistance of 15 to 20 Ω/cm^2, Lumtech Taiwan). Step 1 is the normal spin coating process, during which the substrate is covered by the PEDOT:PSS solution and then is subjected to the spinning process. The PEDOT:PSS aqueous solution with the concentration of 1.3 wt. % in which the weight ratio of PEDOT to PSS is 1:2.5 (Clevios PH1000, Heraeus, Germany) was used as the precursor solution for PEDOT:PSS thin films. PEDOT:PSS thin films with various thicknesses were fabricated by changing the rotation speed or angular velocity at a constant rotation time of 30 s. In selected experiments (when SVPT was used), after spinning, the wet PEDOT:PSS films formed on the ITO-coated glass substrate were promptly placed atop a metal box equipped with an ultrasonic transducer installed inside of the upper surface of the box, vibrating in the vertical direction [Fig. 1(b)]. A function generator drives the piezoelectric ultrasonic transducer at 40 kHz and with variable amplitude or power. The power and duration of the applied vibration highly affect the film characteristics. In this work, the vibration power was set to 5 W and the time was set to 10 s for optimum performance. Excessive vibration power and duration may damage the film. Figure 2 shows the schematic of the entire device and the cross section of a cell obtained by a field emission scanning electron microscope (SEM, Zeiss, Model Zeiss Ultra Plus, Germany). The thickness of the PEDOT:PSS film is about 40 nm when the spin rotation is set to 5000 rpm, indicated by the cross-sectional SEM image as shown in Fig. 2(b). The PEDOT:PSS film thickness fabricated at 3000 and 4000 rpm are estimated to be about 52 and 45 nm, respectively.[30–34] After the deposition of PEDOT:PSS solution, whether with or without ultrasonic vibration, the film was dried at 120°C for 30 min.

P3HT and PCBM powders were purchased from J&K Scientific, China, and used as-received. The P3HT and PCBM in a weight ratio of 1:0.8 were mixed and dissolved in

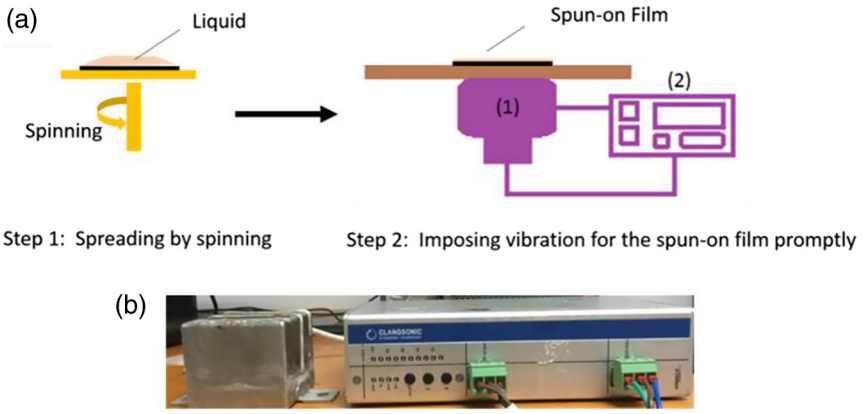

Fig. 1 (a) Schematic of the spin coating process combined with SVPT. The device to impose vertical vibration during spin coating (b) consists of an ultrasonic vibration transducer metal box [left, also labeled as (1) in part (a)] and a function generator [right, also labeled as (2) in part (a)].

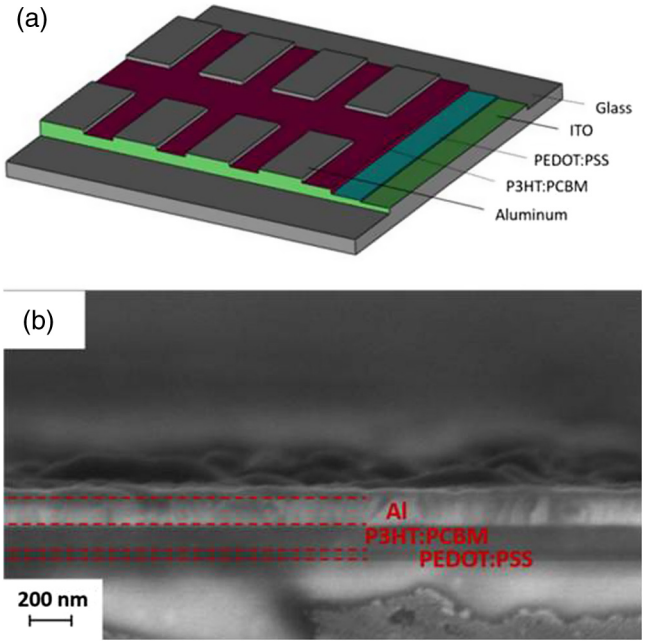

Fig. 2 (a) Schematic of the solar cells fabricated based on the glass/ITO/PEDOT:PSS/P3HT:PCBM/Al architecture. (b) SEM cross-sectional image of a cell. In this cell, the PEDOT:PSS with the thickness of ca. 40 nm was spin-coated using 5000 rpm for 30 s. The thickness of the P3HT:PCBM and Al layers is estimated to be 120 nm.

chlorobenzene to make a solution with the concentration of 27 mg/ml. Before deposition, the solution was stirred overnight and filtered using a 0.45-μm filter. All P3HT:PCBM films were deposited atop PEDOT:PSS films by conventional spin coating at 800 rpm for 12 s and then annealed at a temperature of 125°C for 10 min. To complete the device, using a mask, aluminum with a thickness of about 100 nm was thermally evaporated atop the P3HT:PCBM film to make several electron-extracting-layer free cells on a single substrate, as shown in Fig. 2(a).

Surface topography of thin films and device cross-section were studied by SEM, as mentioned above. The 3D height images of thin films were obtained by atomic force microscopy (AFM, Dimension Icon and FastScan Bio, Brucker, Germany). Optical microscopy images were taken by a confocal laser scanning microscope (CLSM 700, ZEISS, Oberkochen, Germany). To test the photovoltaic performance of the device, the current density–voltage ($J-V$) curves were obtained using Labview and a source meter (model NI PXI-1033, National Instruments, Texas) under illumination from a 500 W solar simulator with an AM1.5G standard filter and intensity of 1000 W/m^2. A standard silicon solar cell was used to calibrate the solar simulator. The cell fabrication, except for the aluminum deposition, was performed in an N_2-filled glovebox, while the photovoltaic performance tests were performed in ambient air. The device incident photon to charge carrier efficiency (IPCE) spectra were obtained by a quantum efficiency measurement system (QEPVSI-b, Newport), showing the external quantum efficiency (EQE) of the device.

3 Results and Discussion

To evaluate the reproducibility of the cell fabrication process, here we report the distribution of photovoltaic performance of devices fabricated under the same conditions, using two routes, i.e., the cells fabricated using conventional spin coating, and the cells fabricated using imposed vibration on wet PEDOT:PSS films to improve the film uniformity and structure. As shown in Fig. 2, using a mask, 6 to 8 cells were made on a substrate, where the effective active area of each cell varies in the range of 0.15 to 0.21 cm^2. Then the data associated with two glass substrates that include 12 to 16 cells were collected to prepare the distribution plots. In the following in Secs. 3.1 and 3.2, the reproducibility of the cells fabricated by conventional spin coating and spin coating followed by SVPT are reported and discussed.

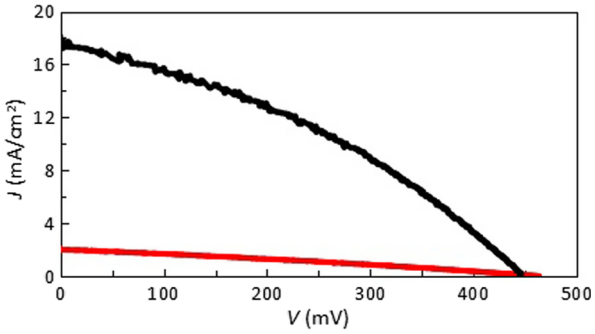

Fig. 3 Typical $J - V$ curves of the cells; shown are the curves for the cells fabricated under the same conditions (PEDOT:PSS was spun at 5000 rpm without vibration). The upper curve corresponds to the PCE of 2.82% and the lower curve corresponds to the worst cell excluding the failed cells.

3.1 *Solar Cells Made Using Conventional Spin Coating*

Figure 3 shows representative $J - V$ curves of the cells fabricated using conventional spin coating. In these cases, the cells were fabricated under the same conditions, where the PEDOT:PSS film was spun at the rotation speed of 5000 rpm and vibration was not imposed. All P3HT:PCBM films were deposited atop PEDOT:PSS films by conventional spin coating using the same spinning condition as reported in Sec. 3. The better curve is the $J - V$ plot of the cell with PCE of 2.82%, while the dashed curve corresponds to the cell with the worst PCE, excluding the failed cells. The better curve shows that the current density J decreases largely with an increase in V indicating the low fill factor (FF) of the device, which is calculated to be 0.36, smaller than about 0.6 which corresponds to a 4% PCE listed in Table 2 from Ref. 3. A low FF is usually attributed to high series resistance. The series resistance is comprised of the film resistance as well as the contact resistance. Another reason for a low FF in this work may be due to cell degradation during the $J - V$ measurements, as a result of exposure to light, water, oxygen, and high temperature, because our tests were carried out in air rather than in N_2-filled glovebox used by Li et al.[3]

Figure 4 shows the photovoltaic performance distribution of cells fabricated without using imposed substrate vibration during deposition of PEDOT:PSS films spun at 5000 rpm. Data from 14 cells were used, in which cells 1 to 7 are associated with the first substrate and 8 to 14 are associated with the second substrate. Parameters used to characterize the photovoltaic performance include the short-circuit current density (J_{sc}), open-circuit voltage (V_{oc}), FF, and PCE. The data for cell No. 3 were excluded because this cell was defected with zero J_{sc}. Figure 4(a) shows the distribution plots of J_{sc} and V_{oc}. The J_{sc} values are scattered, among which the minimum J_{sc} is 0 in cell No. 3 (failed and, therefore, was excluded from the plot), while the maximum J_{sc} is 17.67 mA/cm^2 in cell No. 5. In addition to the cell No. 3 with zero J_{sc}, three other cells, i.e., cell Nos. 2, 10, and 11, show very low J_{sc} values, indicating current leakage in these cells, perhaps due to the presence of pinholes in at least one layer of those cells and,

Table 2 Photovoltaic performance of cells fabricated with and without SVPT at various spinning speeds for making PEDOT:PSS films. The maximum (max) and minimum (min) PCE among the cells fabricated under the same condition are reported.

	Without vibration						With vibration					
	3000 rpm		4000 rpm		5000 rpm		3000 rpm		4000 rpm		5000 rpm	
	Max	Min	Max	Min	Max	Min	Max	Min	Max	Min	Max	Min
PCE (%)	2.17	0.39	2.97	0.11	2.82	0	2.05	0.56	2.51	1.08	2.88	1.01
J_{sc} (mA/cm^2)	13.3	3.22	18.7	1.5	17.7	0	15.4	4.89	17.7	9.47	16.7	6.93
FF	0.37	0.39	0.35	0.17	0.36	—	0.32	0.29	0.34	0.32	0.39	0.30

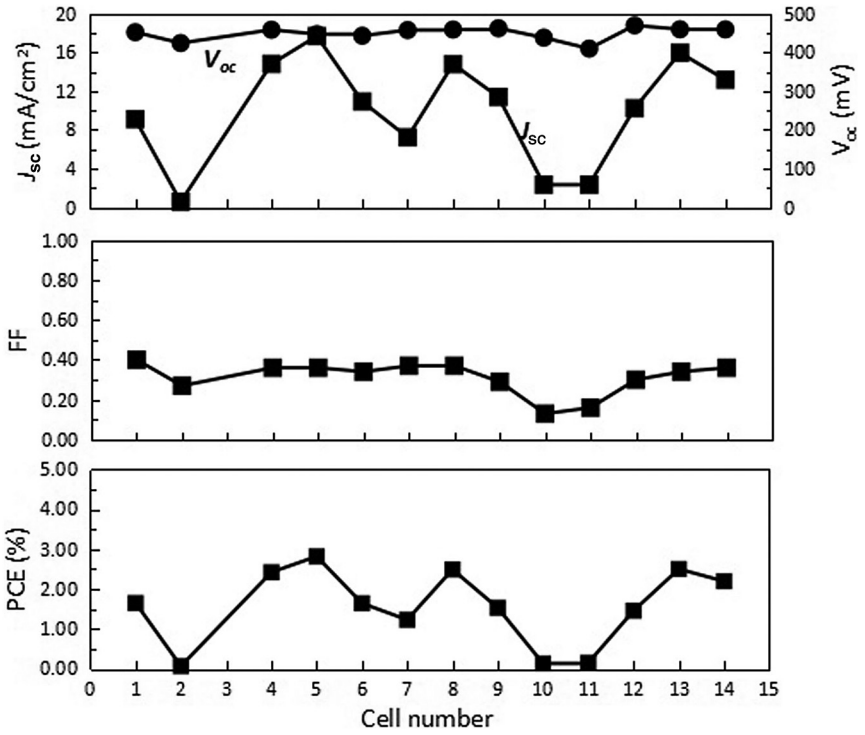

Fig. 4 Photovoltaic performance distribution of several cells fabricated under the same experimental conditions without the assistance of imposed vibration (SVPT) for the fabrication of the spun-on PEDOT:PSS film. In this case, the rotation speed is 5000 rpm. Data from 14 cells were used, in which cell Nos. 1 to 7 are associated with the first substrate, and the rest are associated with the second substrate.

therefore, a low shunt resistance. Cell Nos. 2 and 3 are on one substrate, whereas cell Nos. 9 and 10 are on the second substrate. It is found that the scattered variation in J_{sc} of cell Nos. 1 to 7 on one substrate is somewhat similar to that of the cell Nos. 8 to 14 fabricated on the second substrate. In contrast, the values of V_{oc} are relatively consistent with negligible variation; the values vary from 409 mV in the cell No. 11 to 462 mV in cell No. 9, if the V_{oc} of the defected cell No. 2 with zero short-circuit current is discarded. The V_{oc} is known to be dependent on the energy level between the donor and the acceptor, which for the chosen polymer solar cell structure varies from 400 to about 600 mV, affected by thermal annealing,[3,10–12] and is independent of the thickness of the active layer.[8,9] The V_{oc} is independent of the roughness of the film, as well, for instance, for spray-on cells, the V_{oc} of 580 mV has been reported for the cells fabricated at different process parameters.[35,36] Thus, the results of Fig. 4(a) showing that the average V_{oc} is around 450 mV, even when the J_{sc} is low due to charge recombination and imperfections in the film structure are reasonable.

Figure 4(b) shows the distribution of the FF for the cells fabricated using conventional spin coating. It is observed that the three cells mentioned above with low J_{sc}, i.e., No. 2, 9, and 10, have low FF, as well. Comparison of the FF with J_{sc} plots shows that a higher FF does not necessarily correspond to a higher J_{sc}. Usually, in the published papers on spun-on cells based on P3HT:PCBM, higher FF corresponds to higher J_{sc}, which can be improved by thermal annealing.[3,10–12] However, the reported data in the literature usually correspond to the best devices with uniform and intact films, while our data include all devices and therefore are more reliable for drawing conclusions. The low J_{sc} in cell No. 7 is attributed to the pinholes in the films and thus the relatively high FF of the same cell may indicate that the FF is more dependent on the uniformity of the film rather than the integrity and intactness of the film.

The distribution and scattering of PCE of a group of cells made by conventional spin coating are shown in Fig. 4(c). The highest PCE is 2.82%, which is associated with cell No. 5. It is observed that the values of the PCE are as scattered as the values of J_{sc}. As discussed above, J_{sc} is dependent on the level of intactness and perfection of the thin films (absence

of pinholes), the thickness and nanostructure of the buffer and active layers at micrometer and nanometer scales, and the contact between the adjacent layers. Therefore, the low values and scattering found in PCE are attributed to the lack of adequate uniformity of the layers (low FF) and the presence of random defects and pinholes (scattered J_{sc}), resulted from the solution processing and casting fabrication process. Therefore, this results in lack of reproducibility in the fabrication of spun-on polymer solar cells, although spin coating is known as the most reproducible method for solution-processed solar cells.[10,37,38]

3.2 *Solar Cells Made Using Spin Coating Followed by Ultrasonic Substrate Vibration*

To improve the reproducibility of the solar cells made by conventional spin coating reported in Fig. 4, a new series of similar cells were fabricated, but their PEDOT:PSS layers were subjected to SVPT to homogenize and smooth this layer. Table 2 lists the photovoltaic performance of the cells made without and with vibration, where the maximum and minimum PCE of a group of cells fabricated under the same process conditions are shown. The effect of varying the spinning speed used to fabricate the PEDOT:PSS layer is also explored.

Table 2 shows that without the imposed vibration, when the rotation speed for the fabrication of PEDOT:PSS varies from 3000 to 4000 and 5000 rpm, the maximum PCEs are 2.17%, 2.97%, and 2.82%, respectively. The rotation speed is inversely proportional to the film thickness. The SEM cross-sectional image of the device (c.f., Fig. 2) reveals that the thickness of PEDOT:PSS is about 40 nm, when the rotation speed is 5000 rpm. The thicknesses at 3000 and 4000 rpm are, therefore, estimated to be about 52 and 45 nm, respectively.[30–34] In the literature reports, the optimum thickness for PEDOT:PSS layer is about 30 nm, e.g., Ref. 3; however, here the highest PCE is obtained at a thickness of about 45 nm. A thinner PEDOT:PSS film can be beneficial to reduce the device series resistance. However, a thinner film is also susceptible to excessive defects and pinholes, deteriorating the device performance, corroborated by the data shown in Table 2, which shows that the minimum PCE decreases with an increase in the rotation speed (a decrease in the film thickness). Therefore, a trade-off between the above-mentioned two factors (lower series resistance of thinner films versus lower density of pinholes of thicker films) has to be made to achieve the best device performance. In contrast, under certain conditions, with the application of vibration, the maximum PCE is lower or very close to that without vibration; on the other hand, the minimum PCE of the cells fabricated using vibration are better than those fabricated without vibration, which is an indication of reduced density of pinholes and improved reproducibility of the cells.

Comparison of the photovoltaic performance of several cells fabricated using imposed ultrasonic substrate vibration on PEDOT:PSS films with cells fabricated without vibration is shown in Fig. 5. The histogram showing the distribution of the data in Fig. 5 is shown in Fig. 6. Figure 5 clearly shows a significant improvement in reproducibility of the photovoltaic performance of the cells made using SVPT, compared with those made using conventional spin coating. The histogram shows that in the range of the low photovoltaic performance, which corresponds to the J_{sc} less than 5 mA/cm^2 or PCE less than 1.0, the frequency is 30% among the cells made without vibration, whereas, it is zero among the cells made using vibration, demonstrating that imposing vibration reduces or eliminates the chance for cell failure. On the other hand, at the higher range corresponding to PCE higher than 2.0%, the frequency of the cells fabricated using vibration is higher than those made without vibration.

The average value and standard deviation (STD) of the data of Table 2 and Fig. 5 are plotted in Fig. 7, showing the J_{sc}, FF, and PCE, versus the rotation speed of spin coating of PEDOT:PSS layer. Figure 7 shows that although the maximum PCE without vibration may be slightly higher than that with vibration (cf., Fig. 5), the average values of PCEs made with imposed vibration are higher than those made without vibration, substantiating the positive effect of imposed ultrasonic substrate vibration on reproducibility of the fabrication process, supported also by a decrease in the STD of the cells fabricated using vibration. Our previous results[28] show that the imposed vibration on the substrate has several distinct beneficial effects on the nanostructure and topography of PEDOT:PSS thin films. Imposing a mild vibration for a short duration improves the film uniformity, eliminates excessive pinholes, and increases the electrical conductivity by creating

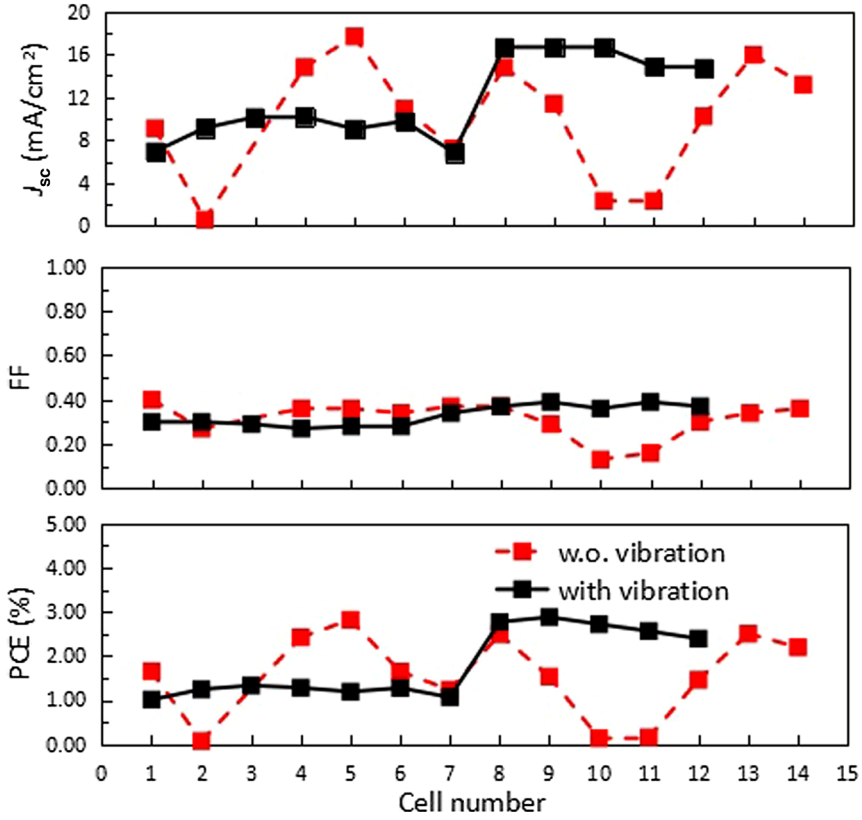

Fig. 5 Comparison of the photovoltaic performance of several cells fabricated with imposed vibration (SVPT) on PEDOT:PSS films with cells fabricated without vibration. In all cases, the rotation speed for PEDOT:PSS film is 5000 rpm. All cells were fabricated under similar process conditions, except for the substrate vibration, which was applied on selected substrates, as shown. Data from 14 cells were used, in which Nos. 1 to 7 are associated with the first substrate, and the rest are associated with the second substrate.

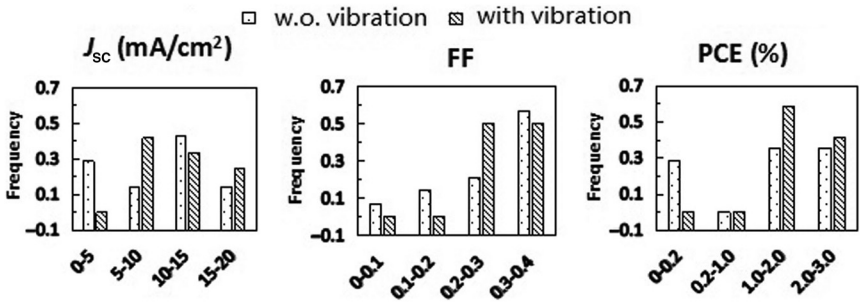

Fig. 6 Histogram of the photovoltaic performance of several cells fabricated with imposed vibration on PEDOT:PSS films with cells fabricated without vibration. In all cases, the rotation speed for PEDOT:PSS film is 5000 rpm. All cells were fabricated under similar process conditions, except for the substrate vibration, which was applied on selected substrates, as shown. Data from 14 cells were used.

an interlocking network of conducting PEDOT chains that can be detached from PSS under the effect of vibration. To further show the positive effect of the imposed vibration, Fig. 8 shows the optical, SEM, and AFM images, comparing the topography of PEDOT:PSS films made with and without vibration. All images show the positive effect of the imposed vibration on improved uniformity of the films made using SVPT. The optical image of the PEDOT:PSS film made using conventional spin coating shows a pinhole on the film, which is eliminated when the film is treated by SVPT. The AFM image clearly shows a more uniform film when SVPT is

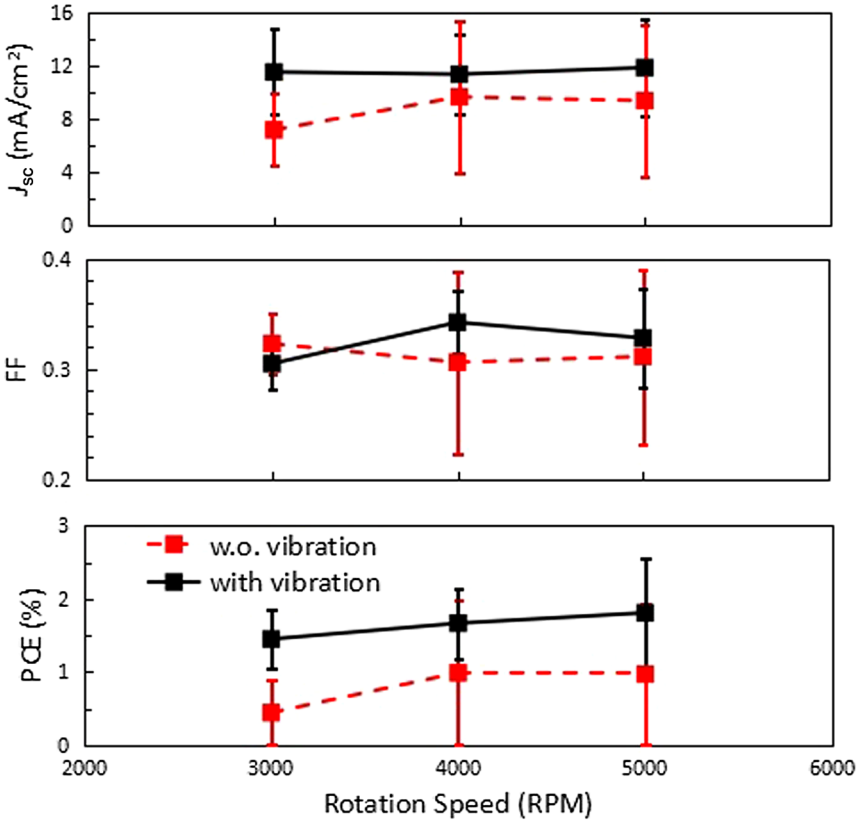

Fig. 7 Photovoltaic performance of a group of solar cells fabricated using conventional spin coating and spin coating followed by SVPT at various rotation speeds used for the fabrication of spun-on PEDOT:PSS films.

applied, in that the vertical variation in the film roughness is significantly reduced. Some spikes appearing in the regular spun-on PEDOT:PSS film are also eliminated when SVPT is applied. This is an indication of reduced pinholes when the film is subjected to ultrasonic vibration.

The effect of ultrasonic SVPT on the cell performance is further elucidated by comparing IPCE, also known as EQE. Figure 9 compares the IPCE or EQE of two representative devices in which their PEDOT:PSS layers were spun at 4000 rpm, one using conventional spin coating and the other using spin coating followed by SVPT, while the other fabrication parameters are identical. The EQE is directly affected by the interfacial and bulk structure of the active and charge transporting layers. Superior EQE observed in the cell fabricated using SVPT [Fig. 9(a)], particularly in blue and green portions of the spectrum, ascertains enhanced collection of both border and deep-generated carriers. This may be attributed to the imposed vibration that results in uniformity of PEDOT:PSS layer, leading to an improvement in interfacial contact between P3HT:PCBM and PEDOT:PSS layers. In addition, the imposed vibration improves the nanostructure and conductivity of PEDOT:PSS,[25–28] thus leading to quick charge depletion from PEDOT:PSS toward the anode and reduced recombination.

The aforementioned results show that imposing ultrasonic vibration on wet spun-on films improves the repeatability of the fabrication process. Our recent unpublished theoretical and experimental results[39] show that the imposed vertical vibration tends to destabilize the thin liquid film, i.e., if the vertical vibration is applied on the liquid film for a long time, the perturbations may grow enough to break up the thin liquid film. On the other hand, imposed vibration creates surface waves that improve the mixing of precursor solution, resulting in a more homogenized solution useful for a homogenized ensuing thin solid film. Given that imposed vibration imparts thermal energy to the liquid film and agitates the film, the solvent evaporation rate increases. This results in a rather rapid curing and drying of the thin liquid film of the precursor solution before the perturbations could break up the film. The overall result is, therefore, an improvement in the film uniformity and functionality, if the vibration power and duration are well controlled.

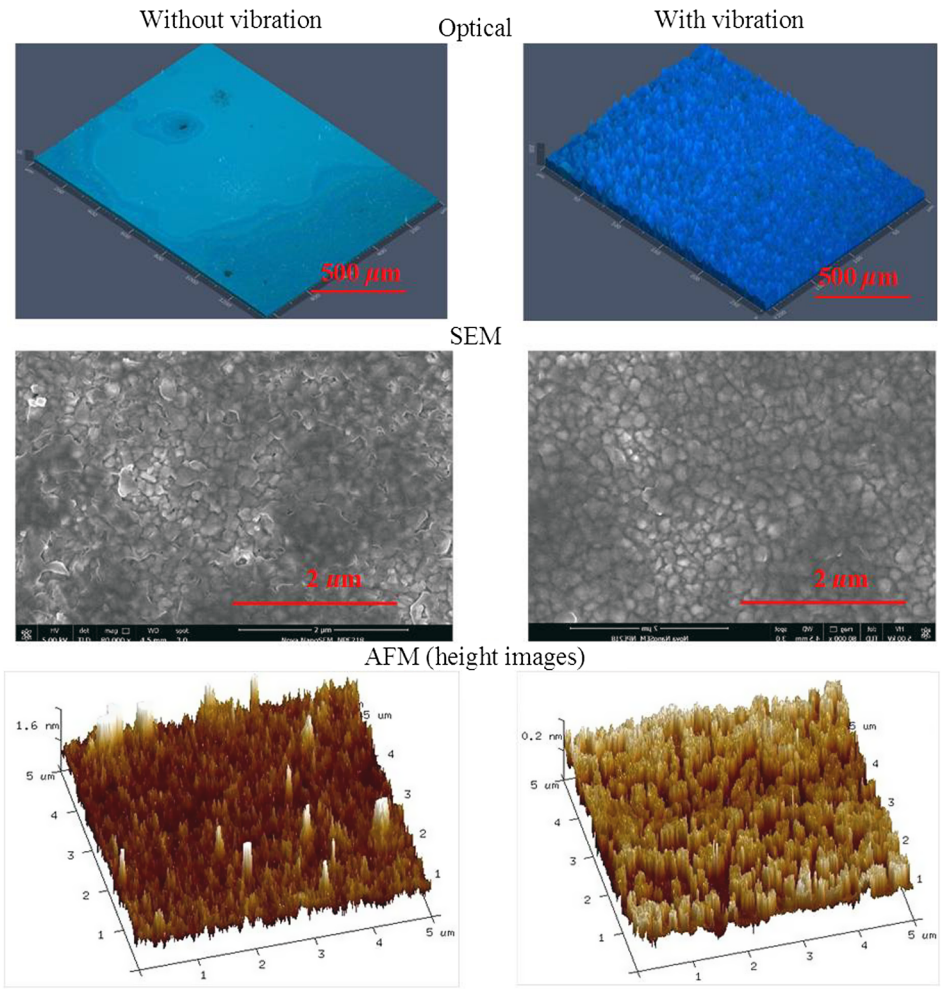

Fig. 8 Microscopic surface morphology of PEDOT:PSS thin films, spun at 5000 rpm. Shown are the optical, SEM, and AFM height images of the films made using (left column) conventional spin coating and (right column) spin coating followed by SVPT.

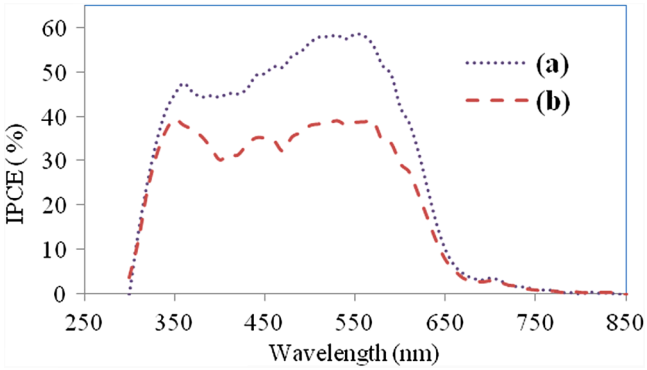

Fig. 9 Effect of ultrasonic SVPT on device IPCE (or EQE). (a) PEDOT:PSS layer was made by spin coating followed by SVPT and (b) PEDOT:PSS layer was made by conventional spin coating. In both cases, PEDOT:PSS layer was spun at 4000 rpm.

It was also observed that although the overall and average performance of the solar cells improve with the application of vibration, the best cell efficiency was obtained in a case without the applied vibration, but it is noted that when vibration is not applied the results are scattered and random and could not be repeated easily by only using basic conventional spin coating without rigorous chemical and thermal posttreatments.

4 Conclusions

In this work, polymer solar cells with the architecture of glass/ITO/PEDOT:PSS/P3HT:PCBM/Al were fabricated by conventional spin coating and spin coating followed by ultrasonic SVPT, applied on the PEDOT:PSS layer only. The ultrasonic vibration was in the vertical direction. The effect of spinning angular velocity and, therefore, the thickness of PEDOT:PSS were studied on the performance of the cells. It was shown that multiple solar cells fabricated using conventional spin coating on a large substrate show scattered performance, mostly in the short-circuit current and PCE. This was attributed to the presence of excessive defects and pinholes in the as-spun films. On the other hand, multiple solar cells fabricated on similar large substrates using spin coating followed by SVPT showed consistent performance, higher average PCE, and EQE, indicating that the SVPT improves the reproducibility of the spun-on solar cells. It is also inferred that the imposed substrate vibration can be combined with scalable methods such as spray coating, to develop scalable and reproducible methods for the fabrication of solution-processed solar cells. In summary, using a simple mechanical treatment, i.e., SVPT eliminates tedious optimization and chemical and thermal treatments steps currently used in the research labs to make the solution-processed solar cells reproducible.

Acknowledgments

Research funding from the Shanghai Municipal Education Commission in the framework of the oriental scholar and distinguished professor designation and funding from the National Natural Science Foundation of China (NSFC) is acknowledged. Y.X. and F.Z. acknowledge research funding from the Postdoctoral Research Foundation of China.

References

1. C. J. Brabec, N. S. Sariciftci, and J. C. Hummelen, "Plastic solar cells," *Adv. Funct. Mater.* **11**, 15–26 (2001).
2. Q. Wang et al., "Progress in emerging solution-processed thin film solar cells–part I: polymer solar cells," *Renewable Sustainable Energy Rev.* **56**, 347–361 (2016).
3. G. Li et al., "Investigation of annealing effects and film thickness dependence of polymer solar cells based on poly(3-hexylthiophene)," *J. Appl. Phys.* **98**, 043704 (2005).
4. C. W. Tang, "Two-layer organic photovoltaic cell," *Appl. Phys. Lett.* **48**, 183–185 (1986).
5. P. Peumans and S. R. Forrest, "Very-high-efficiency double-heterostructure copper phthalocyanine/C60 photovoltaic cells," *Appl. Phys. Lett.* **79**, 126–128 (2001).
6. Q. Zheng et al., "Power conversion efficiency enhancement of polymer solar cells using MoO_3/TFB as hole transport layer," *Appl. Phys. A* **120**, 857–861 (2015).
7. Z. Yuan, "Fabrication, performance and atmospheric stability of inverted ZnO nanoparticle/polymer solar cell," *Appl. Phys. A* **118**, 75–81 (2015).
8. L. Zeng, C. W. Tang, and S. H. Chen, "Effects of active layer thickness and thermal annealing on polythiophene: fullerene bulk heterojunction photovoltaic devices," *Appl. Phys. Lett.* **97**, 053305 (2010).
9. Z. Zhao et al., "Annealing and thickness related performance and degradation of polymer solar cells," *Microelectron. Reliab.* **53**, 123–128 (2013).
10. G. Li et al., "High-efficiency solution processable polymer photovoltaic cells by self-organization of polymer blends," *Nat. Mater.* **4**, 864–868 (2005).
11. M. Reyes-Reyes, K. Kim, and D. L. Carroll, "High-efficiency photovoltaic devices based on annealed poly(3-hexylthiophene) and 1-(3-methoxycarbonyl)-propyl-1-phenyl-(6,6)C61 blends," *Appl. Phys. Lett.* **87**, 083506 (2005).
12. M. Reyes-Reyes et al., "Meso-structure formation for enhanced organic photovoltaic cells," *Org. Lett.* **7**, 5749–5752 (2005).
13. D. Qian et al., "Molecular design toward efficient polymer solar cells with high polymer content," *J. Am. Chem. Soc.* **135**, 8464–8467 (2013).
14. E. Zhou et al., "Control of miscibility and aggregation via the material design and coating process for high-performance polymer blend solar cells," *Adv. Mater.* **25**, 6991–6996 (2013).

15. Y. Lin et al., "A star-shaped perylene diimide electron acceptor for high-performance organic solar cells," *Adv. Mater.* **26**, 5137–5142 (2014).
16. J. Min et al., "Alkyl chain engineering of solution-processable star-shaped molecules for high-performance organic solar cells," *Adv. Energy Mater.* **4**, 1301234 (2014).
17. L. Bian et al., "Recent progress in the design of narrow bandgap conjugated polymers for high-efficiency organic solar cells," *Prog. Polym. Sci.* **37**, 1292–1331 (2012).
18. F. C. Krebs, S. A. Gevorgyan, and J. Alstrup, "A roll-to-roll process to flexible polymer solar cells: model studies, manufacture and operational stability studies," *J. Mater. Chem.* **19**, 5442–5451 (2009).
19. S. Hong et al., "Effect of solvent on large-area polymer-fullerene solar cells fabricated by a slot-die coating method," *Sol. Energy Mater. Sol. Cells* **126**, 107–112 (2014).
20. D. Vak et al., "Fabrication of organic bulk heterojunction solar cells by a spray deposition method for low-cost power generation," *Appl. Phys. Lett.* **91**, 081102 (2007).
21. S. E. Shaheen et al., "Fabrication of bulk heterojunction plastic solar cells by screen printing," *Appl. Phys. Lett.* **79**, 2996–2998 (2001).
22. C. N. Hoth et al., "High photovoltaic performance of inkjet printed polymer: fullerene blends," *Adv. Mater.* **19**, 3973–3978 (2007).
23. F. Zabihi et al., "Morphology, conductivity, and wetting characteristics of PEDOT:PSS thin films deposited by spin and spray coating," *Appl. Surf. Sci.* **338**, 163–177 (2015).
24. Y. Xie, S. Gao, and M. Eslamian, "Characteristics of P3HT:PCBM light harvesting films fabricated by ultrasonic spray coating," *Coatings* **5**, 488–510 (2015).
25. M. Eslamian and F. Zabihi, "Ultrasonic substrate vibration-assisted drop casting (SVADC) for the fabrication of photovoltaic solar cell arrays and thin-film devices," *Nanoscale Res. Lett.* **10**, 462 (2015).
26. M. Habibi et al., "Controlled wetting/dewetting through substrate vibration-assisted spray coating (SVASC)," *J. Coat. Technol. Res.* **13**, 211–225 (2016).
27. F. Zabihi and M. Eslamian, "Substrate vibration-assisted spray coating (SVASC): significant improvement in nano-structure, uniformity, and conductivity of PEDOT:PSS thin films for organic solar cells," *J. Coat. Technol. Res.* **12**, 711–719 (2015).
28. Q. Wang and M. Eslamian, "Improving uniformity and nanostructure of solution-processed thin films using ultrasonic substrate vibration post treatment (SVPT)," *Ultrasonics* **67**, 55–64 (2016).
29. F. Zabihi, M. R. Ahmadian-Yazdi, and M. Eslamian, "Fundamental study on the fabrication of planar perovskite solar cells using two-step sequential substrate: vibration-assisted spraying coating (2S-SVASC)," *Nanoscale Res. Lett.* **11**, 71 (2016).
30. W. W. Flack et al., "A mathematical model for spin coating of polymer resists," *J. Appl. Phys.* **56**, 1199–1206 (1984).
31. D. E. Bornside, C. W. Macosko, and L. E. Scriven, "Spin coating: one-dimensional model," *J. Appl. Phys.* **66**, 5185–5193 (1989).
32. D. B. Hall, P. Underhill, and J. M. Torkelson, "Spin coating of thin and ultrathin polymer films," *Polym. Eng. Sci.* **38**, 2039–2045 (1998).
33. K. P. Cheung et al., "Substrate effect on the thickness of spin-coated ultrathin polymer film," *Appl. Phys. Lett.* **87**, 214103 (2005).
34. C. W. Extrand, "Spin coating of very thin polymer films," *Polym. Eng. Sci.* **34**, 390–394 (1994).
35. C. N. Hoth et al., "Topographical and morphological aspects of spray coated organic photovoltaics," *Org. Electron.* **10**, 587–593 (2009).
36. Y. Byung-Kwan et al., "Factors to be considered in bulk heterojunction polymer solar cells fabricated by the spray process. Selected topics in quantum electronics," *IEEE J. Sel. Top. Quantum Electron.* **16**, 1838–1846 (2010).
37. D. C. Olson et al., "Hybrid photovoltaic devices of polymer and ZnO nanofiber composites," *Thin Solid Films* **496**, 26–29 (2006).
38. J. You et al., "A polymer tandem solar cell with 10.6% power conversion efficiency," *Nat. Commun.* **4**, 1446 (2013).
39. A. Rahimzadeh and M. Eslamian, "Stability of thin liquid films subjected to ultrasonic vibration and characteristics of the resulting thin solid films," *Chem. Eng. Sci.* (in press).

Yu Xie received her PhD in materials science and engineering from University of Leicester, UK. She is an expert in materials science, both experimental and numerical simulations. She is currently a researcher working on lightweight products in the R&D Center of BaoShan Iron & Steel Co., Ltd., Bao Steel Group, Shanghai, China.

Fatemeh Zabihi received her PhD in chemical engineering from Islamic Azad University, Tehran Science and Research Branch, and specializes in thermal fluid sciences, nanoparticle research, and thin films. She is currently a lecturer at Donghua University, Shanghai, China, teaching and also doing research on perovskite and polymer solar cells.

Morteza Eslamian received his PhD from the University of Toronto. His research focuses on thermal fluid sciences and their applications in materials synthesis, such as thin film photovoltaics, thin liquid films, and spray systems. He is currently an associate professor at the University of Michigan-Shanghai Jiao Tong University Joint Institute and cross appointed in the State Key Lab for Composite Materials, School of Materials Science and Engineering, Shanghai Jiao Tong University.